Photoassociative spectroscopy of longrange states of ultracold 6Li2 and 7Li2

E. R. I. Abraham, N. W. M. Ritchie, W. I. McAlexander, and R. G. Hulet

Citation: The Journal of Chemical Physics **103**, 7773 (1995); doi: 10.1063/1.470296
View online: http://dx.doi.org/10.1063/1.470296
View Table of Contents: http://scitation.aip.org/content/aip/journal/jcp/103/18?ver=pdfcov
Published by the AIP Publishing

Photoassociative spectroscopy of long-range states of ultracold $^6Li_2$ and $^7Li_2$

E. R. I. Abraham, N. W. M. Ritchie, W. I. McAlexander, and R. G. Hulet
Physics Department and Rice Quantum Institute, Rice University, Houston, Texas 77251-1892

(Received 22 June 1995; accepted 7 August 1995)

We have obtained spectra of the high-lying vibrational levels of the $A^1\Sigma_u^+$ and $1^3\Sigma_g^+$ states of both $^6Li_2$ and $^7Li_2$ via photoassociation of colliding ultracold atoms confined to a magneto-optical trap. Because of the low collision energies ($\sim$1 mK), very high spectroscopic resolution is realized, and sensitivity is greatest for the usually difficult to access long-range states. Binding energies relative to the center of gravity of the resolved hyperfine structure are given for the $A^1\Sigma_u^+$ vibrational levels $v=62-88$ for $^6Li_2$ and $v=65-97$ for $^7Li_2$, and the $1^3\Sigma_g^+$ vibrational levels $v=56-84$ for $^6Li_2$ and $v=62-90$ for $^7Li_2$. These are extremely long-range levels with outer classical turning points ranging from 25 a_0 to 220 a_0, where a_0 is the Bohr radius. The spectra arise mainly from *s*-wave collisions, and therefore exhibit little rotational structure. © *1995 American Institute of Physics.*

I. INTRODUCTION

Photoassociative spectroscopy of ultracold atoms has recently been demonstrated to be a powerful tool for probing high-lying vibrational levels of diatomic molecules.[1–10] In this type of spectroscopy, a photoassociating laser beam is passed through a sample of laser-cooled trapped atoms. If its frequency ω_P is tuned to resonance between the unbound state of two colliding atoms and a bound molecular excited state, as in Fig. 1, an excited molecule may be formed. This excited-state molecule may radiatively decay into the unbound continuum of two free atoms or into a bound ground-state molecule. In the former case, the kinetic energy acquired by the free atoms is often sufficient for them to escape a shallow neutral atom trap. Both processes can result in an observable reduction of trapped atoms. In some cases the excited molecule can be photo-ionized or excited into an autoionizing state in a second laser excitation step, resulting in detectable charged particles.[1–4] A molecular spectrum is obtained by scanning ω_P through a range of free-bound resonances. Photoassociative spectroscopy is complementary to traditional bound-bound molecular spectroscopy since the excitation overlap with unbound states is maximum with the usually hard to access high-lying excited levels. Furthermore, energies are measured relative to the dissociation limit, enabling a direct measurement of the dissociation energy. Finally, as first pointed out by Thorsheim *et al.*,[11] photoassociation of ultracold atoms can provide high-resolution molecular spectra because of the low collision energies. For atoms cooled to $T=1$ mK, a spectral resolution of approximately $k_BT/h=21$ MHz may be sufficient to resolve hyperfine structure.

Photoassociative spectroscopy has been used to obtain information on the interactions between atoms to high precision. The observed high-lying levels are particularly sensitive to long-range interaction potentials. Stwalley pointed out many years ago that these long-range molecules have unusual and interesting properties.[12] In the case of a homonuclear diatomic molecule formed of alkali-metal atoms, the long-range potential of a molecular state correlating to a ground *s* state and an excited *p* state atom is predominantly due to a C_3/R^3 resonant dipole interaction, where R is the internuclear separation.[13] The proportionality constant, C_3, which depends on the radial dipole moment between the atomic *s* and *p* states, can be extracted from the photoassociative spectrum. Since the radial dipole moment is in turn related to the atomic radiative lifetime, a *molecular* spectrum can be used to determine an *atomic* lifetime. Such lifetime determinations have been made with a precision of several percent for the first excited *p* states of rubidium[7] and of sodium,[3] and with 0.6% precision in the case of lithium[9] using the data presented in this paper. For the sake of comparison, the most precisely stated direct measurement of any atomic radiative lifetime is that of the Li $2p$ state, for which the stated precision is 0.16%.[14] Unfortunately, the measured value differs by more than four standard deviations from most of the modern theoretical results.[9] This disagreement supplies a motivation for attempting to extract the radial dipole moment from molecular data with greater accuracy.

Photoassociative spectroscopy can also be used to obtain information on ground state interaction potentials. These potentials are expected to significantly affect the behavior of weakly interacting atomic gases near the region of phase space density where Bose–Einstein condensation may occur.[15,16] At sufficiently low temperature, elastic scattering from any potential can be described by a single parameter, the *s*-wave scattering length.[17] Recently, the *s*-wave scattering length for spin-polarized ^{7}Li was determined with high accuracy by using two-photon photoassociative spectroscopy of the $a^3\Sigma_u^+$ ground state of $^7Li_2$.[10] This was the first demonstration of photoassociative spectroscopy of a molecular ground state. The intensities and spectral shapes of one-photon photoassociation features can also provide information about ground state potentials,[4,6,11,18] as was recently demonstrated.[8,19]

In this paper we present photoassociative spectra of the $A^1\Sigma_u^+$ and $1^3\Sigma_g^+$ states of $^6Li_2$ and $^7Li_2$. The binding energies of all observed vibrational and rotational levels are tabulated. A model potential is used to assign exact vibrational quantum numbers. Finally, we use an analysis of the pure long-range potential to extract the $2s$-$2p$ atomic dipole moment, and hence the $2p$ atomic radiative lifetime.

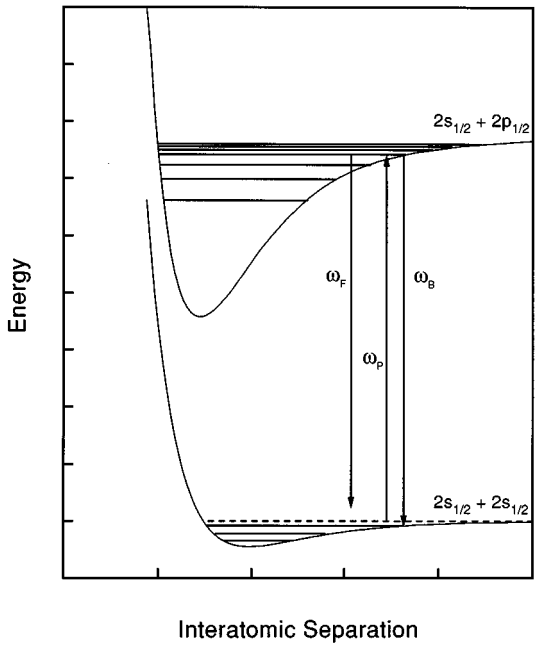

FIG. 1. Schematic showing photoassociation of alkali atoms. As two atoms collide, they absorb a photon of frequency ω_P which is resonant with the free ground state and bound vibrational level of an excited molecular state. The excited molecule can spontaneously decay into an unbound free state by emitting a photon of frequency ω_F, or into a bound ground-state molecule by emitting a photon of frequency ω_B. Since either process leads to a loss of trapped atoms, photoassociation can be observed by monitoring the trap laser induced atomic fluorescence. Potential curves are not given to scale.

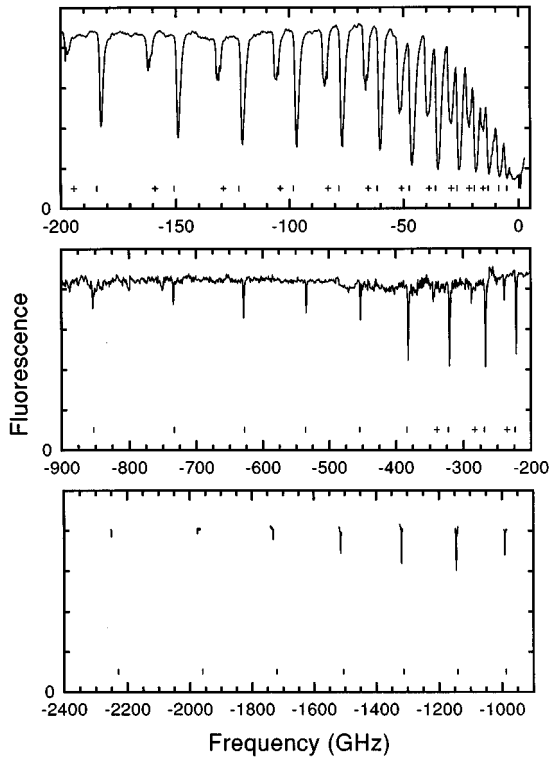

FIG. 2. Photoassociative spectrum of $^7Li_2$. A molecular resonance causes a reduction in the trap laser induced fluorescence. The frequency scale is relative to the $2s_{1/2} \leftrightarrow 2p_{1/2}$ atomic resonance frequency, adjusted to the hyperfine center of gravity. This spectrum is a composite of several individual scans, which have been scaled to display a common fluorescence offset. The relative intensities of lines from different scans are not quantitatively comparable. At larger binding energies, the scans were not continuous. Vibrational levels $v=62$ to $v=90$ are observed for the $1^3\Sigma_g^+$ state; vibrational levels $v=83$ to $v=96$ are evident for the $A^1\Sigma_u^+$ state. Eigenvalues of a model potential are indicated by "|'s" for the $1^3\Sigma_g^+$ levels and "+'s" for the $A^1\Sigma_u^+$ levels. Additional levels have been observed, and binding energies for all are given in Table I.

II. EXPERIMENT

The sample of ultracold lithium atoms was held in a magneto-optical trap,[20] which was loaded from a laser-slowed atomic beam. The apparatus and methods we use to slow and trap lithium have been described in prior publications.[21,22] In the present work, either ^{6}Li or ^{7}Li could be trapped by compensating the laser frequencies for the isotope shift of the $2s_{1/2} \leftrightarrow 2p_{3/2}$ resonance transition frequency ($\sim$10 GHz). The six trap laser beams and the slowing laser beam were derived from a single stabilized ring dye laser offset frequency locked to the lithium resonance line using saturated absorption in a lithium vapor cell. The trap laser beams were frequency modulated using a $LiTaO_3$ standing-wave electric-optic modulator[23] to produce sideband frequencies resonant with transitions from both ground-state hyperfine levels of the Li atom. For ^{7}Li, the modulation frequency of 406.4 MHz produced lower and upper first-order sidebands which were detuned 24 MHz below the $2s_{1/2}$, $F=2 \rightarrow 2p_{3/2}$, $F=3$ and $2s_{1/2}$, $F=1 \rightarrow 2p_{3/2}$, $F=2$ transition frequencies, respectively. For ^{6}Li the modulation frequency of 115.8 MHz produced first-order sidebands which were detuned 37 MHz below the $2s_{1/2}$, $F=3/2 \rightarrow 2p_{3/2}$, $F=5/2$ and the $2s_{1/2}$, $F=1/2 \rightarrow 2p_{3/2}$, $F=3/2$ transition frequencies, respectively. The combined power in the six trap beams in each of the first-order sideband components was approximately 75 mW, and the Gaussian waist (e^{-2} intensity radius) of each beam was approximately 3 mm. The density distribution of trapped atoms was near Gaussian, with a Gaussian radius of 400 μm and a central density of approximately 8×10^{10} cm^{-3} for ^{7}Li, while for ^{6}Li the Gaussian radius was approximately 900 μm with a central density of approximately 5×10^{10} cm^{-3}. The temperature of the trapped atoms was estimated to be 1–2 mK.

A second dye laser was used to produce a laser beam of frequency ω_P which was directed through, and retroreflected back through the trapped atom cloud to induce photoassociation. The photoassociating laser beam had a power of between 450–600 mW and Gaussian waist of between 500–750 μm over the span of time the data were taken. A spectrum was obtained by slowly sweeping ω_P red of the $2s_{1/2} \leftrightarrow 2p_{3/2}$ atomic transition while simultaneously monitoring the trap-laser induced atomic fluorescence with a photodiode. A molecular resonance caused a reduction in the steady-state number of trapped atoms, and a corresponding reduction in detected fluorescence.

A relative frequency scale was obtained by directing a portion of both the photoassociation beam and the trap beam into a calibrated Fabry–Perot etalon. As ω_P was scanned, markers separated by the 1.499 935(85) GHz free spectral range of the etalon were recorded simultaneous with the pho-

TABLE I. Binding energies in GHz relative to the hyperfine center of gravity for the observed rovibrational levels of the $1^3\Sigma_g^+$ and $A^1\Sigma_u^+$ states of $^7Li_2$.

v	$1^3\Sigma_g^+$ $(N=1)$	$A^1\Sigma_u^+$ $(N=0)$	$A^1\Sigma_u^+$ $(N=1)$	$A^1\Sigma_u^+$ $(N=2)$
62	2248.68(13)			
63	1975.33(12)			
64	1731.45(10)			
65	1513.180(89)		4383.86(25)	
66	1318.313(78)		3899.53(22)	
67	1144.790(69)[a]		3460.38(20)	
68	990.678(66)		3063.96(17)	
69	854.208(54)		2706.68(15)	
70	733.652(54)		2385.33(14)	
71	627.566(43)		2096.77(12)	
72	534.472(36)		1838.20(11)	
73	453.089(22)		1607.014(93)	
74	382.161(22)		1400.653(87)	
75	320.605(31)		1217.027(77)	
76	267.430(22)		1053.911(67)	
77	221.651(23)			
78	182.464(25)			
79	149.041(26)		669.701(49)	
80	120.713(26)		571.115(25)	
81	96.836(25)		484.848(29)	
82	76.832(25)	410.607(35)	409.666(22)	407.868(35)
83	60.202(25)		344.301(41)	
84	46.469(25)		287.821(35)	
85	35.219(25)		239.136(25)	237.844(45)
86	26.116(68)	197.981(28)	197.344(22)	196.211(49)
87	18.928(52)	162.249(49)	161.719(29)	160.712(44)
88	13.257(52)	131.903(69)	131.424(23)	
89	8.990(52)	106.263(43)	105.858(30)	105.041(37)
90	5.775(52)	84.789(37)	84.432(30)	83.766(37)
91		66.875(52)	66.553(30)	65.977(36)
92		51.976(85)	51.758(30)	51.274(33)
93		39.868(43)	39.645(30)	39.235(30)
94		30.047(51)	29.835(33)	29.488(36)
95		22.214(52)	22.005(34)	21.719(30)
96		15.990(60)	15.857(33)	15.610(40)
97			11.160(43)	10.952(36)

[a]Rotational structure was resolved only for this vibrational level where the binding energy for the $N=0$ state was 1146.728(73) GHz and for the $N=2$ state, 1141.311(76) GHz.

toassociation spectrum. The frequency scale was calibrated relative to the $2s_{1/2}\leftrightarrow 2p_{1/2}$ atomic resonance frequency. In regions where ω_P was not scanned continuously, a scanning Michelson interferometer wavemeter whose accuracy of 0.5 GHz was sufficient to resolve adjacent etalon fringes, was used to link sets of etalon markers to the $2s_{1/2}\leftrightarrow 2p_{1/2}$ frequency reference.

III. RESULTS

The photoassociative spectrum of $^7Li_2$ is given in Fig. 2. Vibrational levels of a "strong" series are observed with binding energies of up to 2.3 THz (binding "energy" will refer to the corresponding frequency). By comparing with the eigenvalues of a model potential discussed in Section IV, the observed vibrational levels are assigned to $v=62$ to $v=90$ of the $1^3\Sigma_g^+$ state. The "weak" vibrational series observable to binding energies of up to 340 GHz is assigned to the $A^1\Sigma_u^+$ state. Subsequent work has succeeded in observing all the way down to the $v=65$ level of the $A^1\Sigma_u^+$ state,

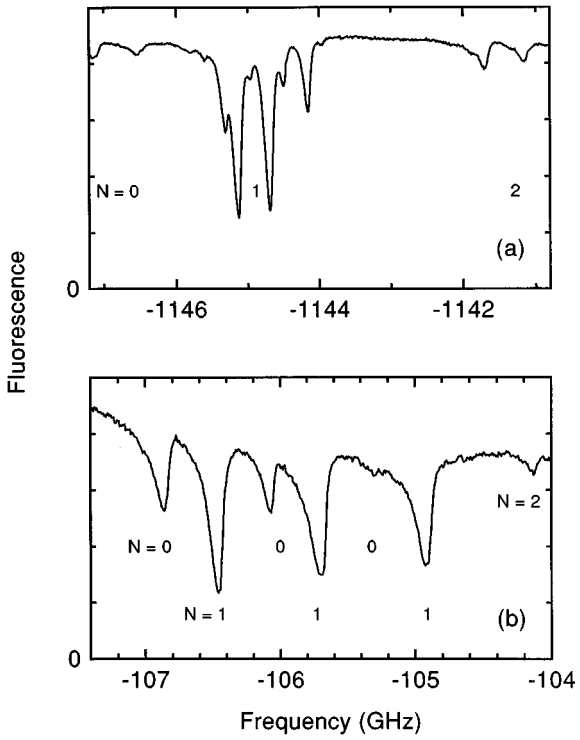

FIG. 3. (a) High resolution spectrum of the $v=67$ level of the $1^3\Sigma_g^+$ state of $^7Li_2$. Three rotational levels corresponding to $N=0$–2 are observed. The complex structure is due to the hyperfine interaction. The $N=1$ feature, which is due predominately to s-wave scattering, is dominant. (b) High resolution spectrum of the $v=89$ level of the $A^1\Sigma_u^+$ state of $^7Li_2$ with resolved hyperfine and rotational structure.

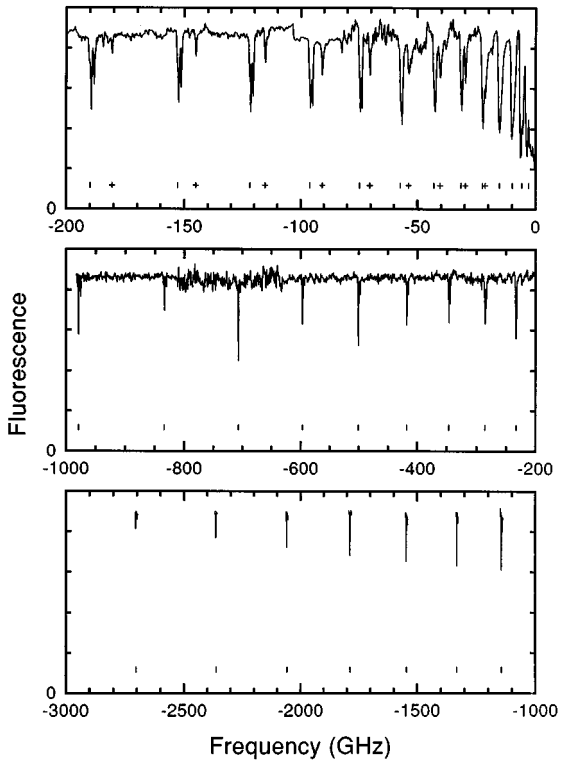

FIG. 4. Photoassociative spectrum of $^6Li_2$. Vibrational levels $v=56$ to $v=84$ are observed for the $1^3\Sigma_g^+$ state; vibrational levels $v=80$ to $v=88$ are observed for the $A^1\Sigma_u^+$ state. Otherwise, the same as Fig. 2.

TABLE II. Binding energies in GHz relative to the hyperfine center of gravity for the observed rovibrational levels of the $1^3\Sigma_g^+$ and $A^1\Sigma_u^+$ states of $^6Li_2$.

v	$1^3\Sigma_g^+$ $(N=0)$	$1^3\Sigma_g^+$ $(N=1)$	$1^3\Sigma_g^+$ $(N=2)$	$A^1\Sigma_u^+$ $(N=0)$	$A^1\Sigma_u^+$ $(N=1)$	$A^1\Sigma_u^+$ $(N=2)$
56		2705.62(16)				
57		2363.63(14)				
58		2058.49(12)				
59	1789.97(17)	1786.95(11)				
60	1548.48(15)	1545.913(93)	1540.94(22)			
61	1334.83(22)	1332.571(82)	1328.06(22)			
62	1146.28(26)	1144.287(72)	1140.08(79)		3459.35(20)	
63	980.47(24)	978.679(64)	975.08(34)		3033.05(17)	
64	835.12(31)	833.445(57)	829.96(34)		2652.10(15)	
65	708.09(13)	706.501(51)	703.42(27)		2312.43(13)	
66	597.48(18)	596.058(47)	593.25(26)		2010.19(11)	
67	501.45(32)	500.247(55)	497.72(43)		1741.918(99)	
68	418.58(24)	417.498(40)	416.81(33)	1506.717(86)	1504.375(85)	
69	347.28(29)	346.343(37)	344.21(22)	1296.582(74)	1294.614(74)	
70	286.24(21)	285.440(51)	283.63(30)	1111.689(63)	1109.895(63)	
71	234.29(22)	233.542(34)	231.80(46)	949.314(55)	947.738(54)	
72	190.28(19)	189.622(33)	188.11(39)		805.809(48)	
73	153.23(12)	152.584(64)	151.43(26)			
74	122.10(19)	121.761(48)	120.54(29)			
75	96.30(18)	95.888(48)	94.99(22)			
76	74.96(18)	74.510(64)	73.82(25)		401.078(24)	
77	57.47(18)	57.097(48)	56.50(22)		332.127(20)	
78	43.30(16)	42.989(23)	42.39(22)		273.247(17)	
79	31.91(16)	31.580(64)	31.09(27)	224.157(19)	223.181(14)	221.767(14)
80		22.608(24)	22.21(21)		180.757(30)	
81		15.69(32)		145.764(59)	145.181(30)	144.112(41)
82		10.34(26)			115.404(35)	
83		6.55(31)		91.202(38)	90.746(23)	89.953(25)[a]
84		4.10(32)		70.820(25)	70.432(23)	69.760(25)
85					53.874(32)	
86					40.470(23)	
87					29.809(16)	
88					21.407(64)	

[a]For this vibrational level, rotational state $N=3$ was observed and has a binding energy of 88.778(30) GHz.

which has a binding energy of 4.4 THz. The binding energies of all rovibrational levels observed for $^7Li_2$ are given in Table I.

A high resolution scan of one vibrational level for each potential is shown in Fig. 3. Rotational levels $N=0-2$ are observed for each state. The dominant feature is $N=1$, which arises mainly from s-wave scattering.[24] Hyperfine structure is resolved for both states. While the $A^1\Sigma_u^+$ excited state does not have hyperfine structure, three features separated by the atomic ground state hyperfine interval of 803.5 MHz are observed due to the possibility of each colliding atom of being in either the $f=1$ or $f=2$ atomic hyperfine level. For the $A^1\Sigma_u^+$ transitions shown, the rotational splitting is comparable to the hyperfine splitting,[25] whose scale is set by the atomic ground state hyperfine interval of 803.5 MHz.

The photoassociative spectrum for $^6Li_2$ is given in Fig. 4. Again, the stronger vibrational series corresponds to the $1^3\Sigma_g^+$state. Levels $v=56-84$ were observed with binding energies of up to 2.7 THz. The weaker series, with binding energies of up to 200 GHz, corresponds to $v=80$ to $v=88$ of the $A^1\Sigma_u^+$ state. Subsequent work has observed vibrational levels as deep as $v=62$ in the $A^1\Sigma_u^+$ state. The binding energies of all observed rovibrational levels of the $1^3\Sigma_g^+$ and $A^1\Sigma_u^+$ states for $^6Li_2$ are given in Table II.

A high resolution scan of one vibrational level for each potential of $^6Li_2$ is shown in Fig. 5. The structure is due to both hyperfine and rotational interactions. The $N=0-2$ rotational levels are clearly evident in Fig. 5(a) for the $1^3\Sigma_g^+$ state. Because the hyperfine interaction is relatively weak for $^6Li_2$, the rotational structure is larger than the hyperfine structure for nearly all vibrational levels observed. For each rotational level for the $A^1\Sigma_u^+$ state, three hyperfine features separated by the atomic ground state hyperfine splitting of 228.2 MHz.

The binding energy is measured from the center of gravity of the hyperfine splitting of the $2s_{1/2}\leftrightarrow 2p_{1/2}$ atomic transition, to the center of gravity of the hyperfine structure for each vibrational level. A complete discussion of the hyperfine structure will be presented in a separate publication.[25] An uncertainty in the binding energies of 10 to 50 MHz comes from the uncertainty in determining the molecular center of gravity due to the spectral width of the individual hyperfine features. For those rovibrational levels where specific hyperfine features are not resolved, the uncertainty in the binding energies is 100–400 MHz, depending on the spectral width of the feature. The calibration of the etalon introduces a relative uncertainty in the binding energy of $\pm 5.7\times 10^{-5}$. This becomes significant compared to the fea-

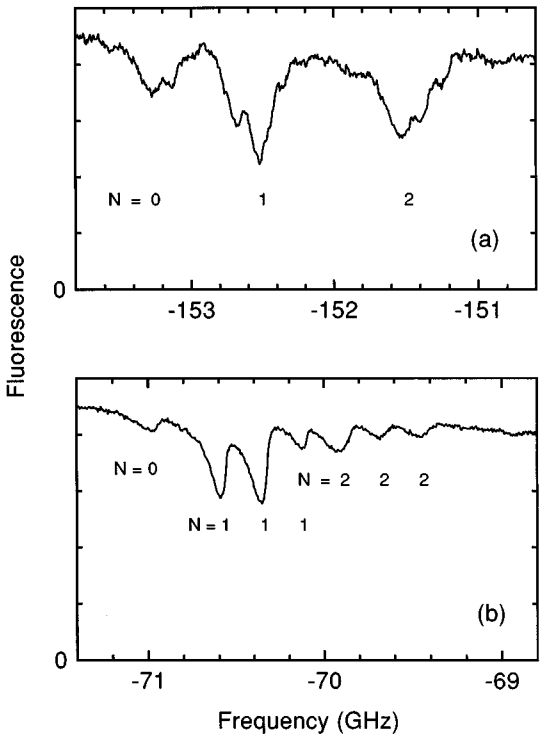

FIG. 5. (a) High resolution spectrum of the $v=73$ level of the $1^3\Sigma_g^+$ state of $^6Li_2$. Three rotational levels are observed corresponding to $N=0$–2. Hyperfine structure is evident within each rotational level. (b) High resolution spectrum of the $v=84$ level of the $A^1\Sigma_u^+$ state of $^6Li_2$ with resolved hyperfine and rotational structure.

ture width only at the largest binding energies.

Previous experiments using $^7Li_2$ have observed the $v=0$–7 vibrational levels for the $1^3\Sigma_g^+$ state,[26] and the $v=0$–26 vibrational levels for the $A^1\Sigma_u^+$ state.[27,28] Recently, vibrational levels 0–62 have been observed for the $A^1\Sigma_u^+$ state using triple resonance molecular spectroscopy.[29] The only vibrational energies previously reported for the $A^1\Sigma_u^+$ and $1^3\Sigma_g^+$ states of $^6Li_2$ were for the $v=0$–7 levels of the triplet state.[26] However, vibrational levels $v=0$–84 were recently recorded using Fourier transform spectroscopy.[30] This data, along with that presented here, are the first reported spectroscopic measurements of the $A^1\Sigma_u^+$ state of $^6Li_2$.

IV. ANALYSIS

To assign the vibrational series, a composite potential was created using spectroscopic data and *ab initio* calculations.[9] The composite potential adopted Rydberg–Klein–Rees (RKR) potential points developed from previous spectroscopic data of the $1^3\Sigma_g^+$ state[26] and the $A^1\Sigma_u^+$ state[27] where available. These points are located around the region of interatomic separation R that includes the potential minimum ($\sim 6a_0$ for both the triplet and singlet states, where a_0 is the Bohr radius). Their uncertainty is determined by the uncertainty of the dissociation energies D_e of the excited states which in turn depend on the uncertainties of D_e of the ground states from which the spectroscopy is referenced. The uncertainties in D_e are found to be ± 0.3 cm^{-1} for the triplet states and ± 0.08 cm^{-1} for the singlet states.[31] This is the most accurately known region of the potential.

For both the inner wall ($R \leqslant 5a_0$) section of the interatomic potential and for R between $10a_0$ and $20a_0$, two different, highly regarded *ab initio* potentials were used. The potentials of Schmidt-Mink *et al.* produce the best comparison with spectroscopically known constants.[32] The average of two *ab initio* calculations by Konowalow *et al.*, for which the expected errors are of opposite sign, is also expected to be a reasonable approximation to the true potential.[33] Since there is not enough evidence to believe one theoretical potential is more accurate than the other in the regions of interest, they are used to make separate potentials and the results of both are compared.

For the long-range interaction region, $R \geqslant 20a_0$, the potential is approximated analytically by an expansion in an inverse power series of R. For the singly excited potentials of Li_2, the appreciable non-vanishing terms of the expansion are

$$V(R) = -\frac{C_3}{R^3} - \frac{C_6}{R^6} - \frac{C_8}{R^8}. \tag{1}$$

The $-C_3/R^3$ term corresponds to the resonant dipole–dipole interaction, while the $-C_6/R^6$ and $-C_8/R^8$ terms represent the dispersion interaction. The C_n coefficients are obtained from several theoretical calculations[34] that vary by $\pm 1.4\%$ for C_3 and $\pm 20\%$ for C_6 and C_8. At very long range, the magnitude of the electronic interaction energy becomes comparable to the atomic spin–orbit interaction, and the coupling changes from Hund's case (b) to case (c). The $A^1\Sigma_u^+$ Hund's case (b) state correlates to the 0_u^+ Hund's case (c) state at very long range, while the $1^3\Sigma_g^+$ state correlates to the 1_g and 0_g^- Hund's case (c) states.[35] The energies of the Hund's case (c) states depend on the p state fine-structure interval as well as on the long-range expansion coefficients C_3, C_6, and C_8 in an analytic way.[35] The composite potential is constructed by joining the separate regions smoothly using a cubic spline fit.

Eigenvalues of the model potentials are calculated and compared to the experimental data. These comparisons verify the assignment of the $1^3\Sigma_g^+$ state to the observed "strong" series and assignment of the $A^1\Sigma_u^+$ state to the observed "weak" series for both isotopes. The potentials are accurate enough to assign absolute vibrational quantum numbers, which was checked by varying each component of the model potential by its respective uncertainty. Even in the extreme case where all the components were systematically shifted so as to generate the greatest swing in the calculated eigenvalues, the vibrational numbers assigned to the experimental spectrum did not change. Furthermore, the vibrational assignments for the two isotopes are consistent with a simple mass scaling.[36] The assignments were also verified by identifying specific hyperfine levels,[25] as was first suggested in Ref. 37.

One application for high-lying spectra is to obtain information about the long-range form of the interaction potential, from which one can extract the atomic lifetime. The coefficient C_3 given in Eq. (1) is proportional to the square of the atomic $2s$-$2p$ dipole matrix element, which is inversely proportional to the $2p$ atomic radiative lifetime, τ, by[13]

$$C_3 = \frac{3\hbar}{2\tau}\left(\frac{\lambda}{2\pi}\right)^3, \tag{2}$$

where λ is the wavelength of the atomic transition. A method for extracting the leading C_n coefficient assuming the pure long-range form of the potential $-C_3/R^3$, was developed in Refs. 38. This method has been applied to ultracold photoassociation spectra of sodium[3] and rubidium,[7] from which C_3 coefficients were extracted with an uncertainty of several percent.

This analysis ignores the other terms of the long-range expansion given in Eq. (1) and the variation of the inner part of the potential as a function of energy. A modification of the long-range analysis was done by LeRoy,[39] to incorporate the higher order long-range terms. LeRoy's equation can be solved for C_3 numerically using an iterative procedure. We applied this process to the $N=0$, $1^3\Sigma_g^+$ state of $^6Li_2$ and found $C_3 = 11.09$ atomic units, corresponding to a radiative lifetime of 26.88 ns. This result is consistent with a previous calculation using the entire model potential which gave a value of 26.99 ± 0.16 ns.[9] A method which utilizes the entire potential, such as that of Ref. 9 or takes the inner part of the potential into account by fitting for an energy dependent phase,[40] is expected to be more accurate. However, in cases where the inner part of the potential is not well known, this method can be used to obtain an approximate value.

V. CONCLUSIONS

We have obtained high-lying vibrational spectra of previously unobserved levels of the $A^1\Sigma_u^+$ and $1^3\Sigma_g^+$ states of $^6Li_2$ and $^7Li_2$ via photoassociative spectroscopy of ultracold atoms. Because of the low collision energies there is very high spectral resolution and little rotation. Consequently, the hyperfine structure is largely resolved, aiding in the precise determination of binding energies. In a prior publication, the $2p$ radiative lifetime was extracted from the data with an uncertainty of 0.6%.[9] This uncertainty is insufficient to resolve the four standard deviation discrepancy between direct measurements and calculations of this lifetime. However, our current ability to extract the lifetime is not limited by the spectroscopic precision, but rather uncertainties in the model potential, particularly in the region between 10 a_0 and 20 a_0. This situation could be improved by better *ab initio* calculation or by more spectroscopic data on lower lying states. New spectroscopic data on the $A^1\Sigma_u^+$ state of $^7Li_2$, up to $v=62$,[29] and the $A^1\Sigma_u^+$ state of $^6Li_2$ up to $v=84$,[30] coupled with the data presented here may dramatically improve this situation.

ACKNOWLEDGMENTS

We gratefully acknowledge helpful discussions with P.S. Julienne and C.J. Williams. This work has been supported by the National Science Foundation, the Texas Advanced Technology Program, and the Robert A. Welch Foundation. W.I.M. received support from the Fannie and John Hertz Foundation.

[1] V. Bagnato, L. Marcassa, C. Tsao, Y. Wang, and J. Weiner, Phys. Rev. Lett. **70**, 3225 (1993).
[2] V. S. Bagnato, J. Weiner, P. S. Julienne, and C. J. Williams, Laser Phys. **4**, 1062 (1994).
[3] P. D. Lett, K. Helmerson, W. D. Phillips, L. P. Ratliff, S. L. Rolston, and M. E. Wagshul, Phys. Rev. Lett. **71**, 2200 (1993).
[4] L. P. Ratliff, M. E. Wagshul, P. D. Lett, S. L. Rolston, and W. D. Phillips, J. Chem. Phys. **101**, 2638 (1994).
[5] P. D. Lett, P. S. Julienne, and W. D. Phillips, Annu. Rev. Phys. Chem. **46**, 423 (1995).
[6] J. D. Miller, R. A. Cline, and D. J. Heinzen, Phys. Rev. Lett. **71**, 2204 (1993).
[7] R. A. Cline, J. D. Miller, and D. J. Heinzen, Phys. Rev. Lett. **73**, 632 (1994).
[8] J. R. Gardner, R. A. Cline, J. D. Miller, D. J. Heinzen, H. M. J. M. Boesten, and B. J. Verhaar, Phys. Rev. Lett. **74**, 3764 (1995).
[9] W. I. McAlexander, E. R. I. Abraham, N. W. M. Ritchie, C. J. Williams, H. T. C. Stoof, and R. G. Hulet, Phys. Rev. A **51**, R871 (1995).
[10] E. R. I. Abraham, W. I. McAlexander, C. A. Sackett, and R. G. Hulet, Phys. Rev. Lett. **74**, 1315 (1995).
[11] H. R. Thorsheim, J. Weiner, and P. S. Julienne, Phys. Rev. Lett. **58**, 2420 (1987).
[12] W. C. Stwalley, Contemp. Phys. **19**, 65 (1978).
[13] G. W. King and J. H. Van Vleck, Phys. Rev. **55**, 1165 (1939).
[14] A. Gaupp, P. Kuske, and H. J. Andrä, Phys. Rev. A **26**, 3351 (1982).
[15] A. L. Fetter and J. D. Walecka, *Quantum Theory of Many-Particle Systems* (McGraw-Hill, New York, 1971).
[16] H. T. C. Stoof, Phys. Rev. A **49**, 3824 (1994).
[17] Cf. K. Huang, *Statistical Mechanics*, 2nd ed. (Wiley, New York, 1987).
[18] R. Napolitano, J. Weiner, C. J. Williams, and P. S. Julienne, Phys. Rev. Lett. **73**, 1352 (1994).
[19] R. Côté, A. Dalgarno, Y. Sun, and R. G. Hulet, Phys. Rev. Lett. **74**, 3581 (1995).
[20] E. L. Raab, M. Prentiss, A. Cable, S. Chu, and D. E. Pritchard, Phys. Rev. Lett. **59**, 2631 (1987).
[21] C. C. Bradley, J. G. Story, J. J. Tollett, J. Chen, N. W. M. Ritchie, and R. G. Hulet, Opt. Lett. **17**, 349 (1992).
[22] N. W. M. Ritchie, E. R. I. Abraham, Y. Y. Xiao, C. C. Bradley, R. G. Hulet, and P. S. Julienne, Phys. Rev. A **51**, R890 (1995).
[23] J. F. Kelly and A. Gallagher, Rev. Sci. Instrum. **58**, 563 (1987).
[24] M. Mizushima, *The Theory of Rotating Diatomic Molecules* (Wiley, New York, 1975).
[25] E. R. I. Abraham, W. I. McAlexander, H. T. C. Stoof, and R. G. Hulet (unpublished).
[26] C. Linton, T. L. Murphy, F. Martin, R. Bacis, and J. Verges, J. Chem. Phys. **91**, 6036 (1989).
[27] P. Kusch and M. M. Hessel, J. Chem. Phys. **67**, 586 (1977).
[28] B. Barakat, R. Bacis, F. Carrot, S. Churassy, P. Crozet, and F. Martin, Chem. Phys. **102**, 215 (1986).
[29] K. Urbanski, S. Antonova, A. Yiannopoulou, A. M. Lyyra, L. Li, and W. C. Stwalley (unpublished).
[30] C. Linton, F. Martin, A. J. Ross, I. Russier, P. Crozet, S. Churassy, and R. Bacis (unpublished).
[31] W. T. Zemke and W. C. Stwalley, J. Phys. Chem. **97**, 2053 (1993).
[32] I. Schmidt-Mink, W. Müller, and W. Meyer, Chem. Phys. **92**, 263 (1985).
[33] M. L. Olson and D. D. Konowalow, Chem. Phys. **21**, 393 (1977); D. D. Konowalow and M. L. Olson, J. Chem. Phys. **71**, 450 (1979); D. D. Konowalow and J. L. Fish, Chem. Phys. **77**, 435 (1983); D. D. Konowalow and J. L. Fish, *ibid*. **84**, 463 (1984); D. D. Konowalow, R. M. Regan, and M. E. Rosenkrantz, J. Chem. Phys. **81**, 4534 (1984).
[34] B. Bussery and M. Aubert-Frécon, J. Chem. Phys. **82**, 3224 (1985), and references therein.
[35] M. Movre and G. Pichler, J. Phys. B **10**, 2631 (1977).
[36] W. C. Stwalley, J. Chem. Phys. **63**, 3062 (1975).
[37] C. J. Williams and P. S. Julienne, J. Chem. Phys. **101**, 2634 (1994).
[38] R. J. LeRoy and R. B. Bernstein, J. Chem. Phys. **52**, 3869 (1970); R. J. LeRoy, Mol. Spectrosc. **1**, 113 (1973); W. C. Stwalley, Chem. Phys. Lett. **6**, 241 (1970).
[39] R. J. LeRoy, J. Chem. Phys. **73**, 6003 (1980).
[40] A. J. Moerdijk, W. C. Stwalley, R. G. Hulet, and B. J. Verhaar, Phys. Rev. Lett. **72**, 40 (1994).